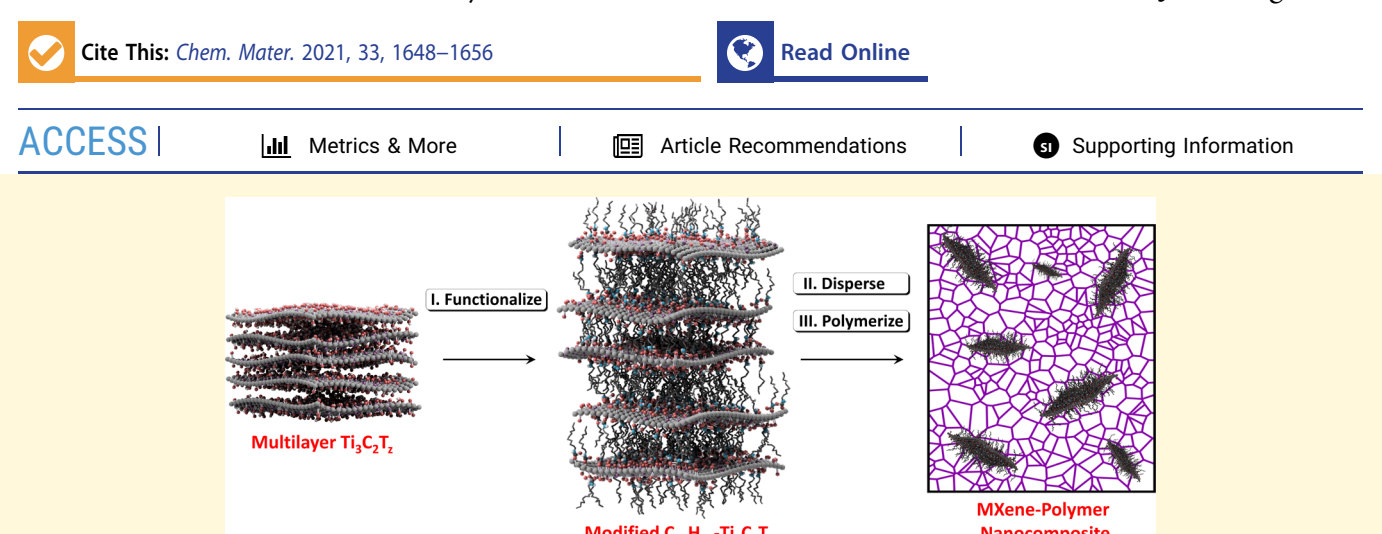


pubs.acs.org/cm Article

# Well-Dispersed Nanocomposites Using Covalently Modified, Multilayer, 2D Titanium Carbide (MXene) and In-Situ "Click" Polymerization

Riki M. McDaniel, Michael S. Carey, Olivia R. Wilson, Michel W. Barsoum, and Andrew J. D. Magenau\*



ABSTRACT: Despite the excellent mechanical and electrical performance of MXene—polymer nanocomposites, methods for producing these materials on a larger scale are limited by low-yielding, delaminated, MXene suspensions that are typically employed for their synthesis. Moreover, the hydrophilicity of MXenes restricts the production of well-dispersed nanocomposites with many polymer matrices. In this contribution, we address such limitations and report, for the first time, a simple method to covalently modify multilayered  $T_{i_3}C_2T_z$  MXenes with isocyanates, which enables their successful dispersion within a hydrophobic thiourethane matrix. The efficacy of our covalent modification was determined to yield high levels of surface grafts and suggests quantitative conversion of the oxygen-containing terminations. *In situ*-polymerized thiourethane "click" matrices were used to demonstrate the utility of this modification for accessing well-dispersed nanocomposites under ambient conditions. The ease of producing modified, multilayered, MXenes at scale and the availability of a wide variety of isocyanates render this method scalable and highly modular. Furthermore, the reported isocyanate treatment was found to be a valuable tool for easily quantifying the concentration of reactive (oxygen-containing) terminations on MXene surfaces.

# ■ INTRODUCTION

MXenes are a versatile family of two-dimensional, 2D, transition-metal carbides/nitrides defined by their  $M_{n+1}X_nT_z$ chemistry, where M is an early transition metal, X is carbon and/or nitrogen, and T represents surface terminations such as −O, −OH, or −F. MXenes can be synthesized and employed as multilayer stacks or delaminated sheets in colloidal suspension. The former MXenes are produced by chemically etching an "A" element (typically Al) from the parent MAX phase  $(M_{n+1}AX_n)$  under acidic conditions. Afterward, the multilayer MXenes can be exfoliated into a few- or single-layer flakes through agitation, intercalation of large cationic species, or by a combination of these two methods. Since their discovery in 2011,<sup>2</sup> MXenes have garnered significant research attention and found wide utility as nanomaterials for electromagnetic shielding,3 energy storage,4 transparent conductors,<sup>5</sup> catalysis,<sup>6</sup> biomaterials,<sup>7</sup> and many other applications because of their advantageous and diverse chemical and physical properties.

Like other 2D nanomaterials, MXenes have shown great promise as fillers for polymer nanocomposites (NCs). Titanium carbide ( $Ti_3C_2T_z$ ) MXene–polymer NCs have been synthesized using a variety of methods including melt-processing, dip-coating, electrospinning, and freeze-drying, but they are most commonly produced by adding hydrophilic polymers to aqueous suspensions of delaminated  $Ti_3C_2T_z$ , followed by filtration. Nanocomposites from  $Ti_3C_2T_z$  have been produced as filtered films using numerous polymers, including sodium alginate, polypyrrole, poly(3,4-ethylenedioxythiophene)—poly(styrene sulfonate), 13,14 polya-

Received: October 9, 2020 Revised: December 29, 2020 Published: January 22, 2021





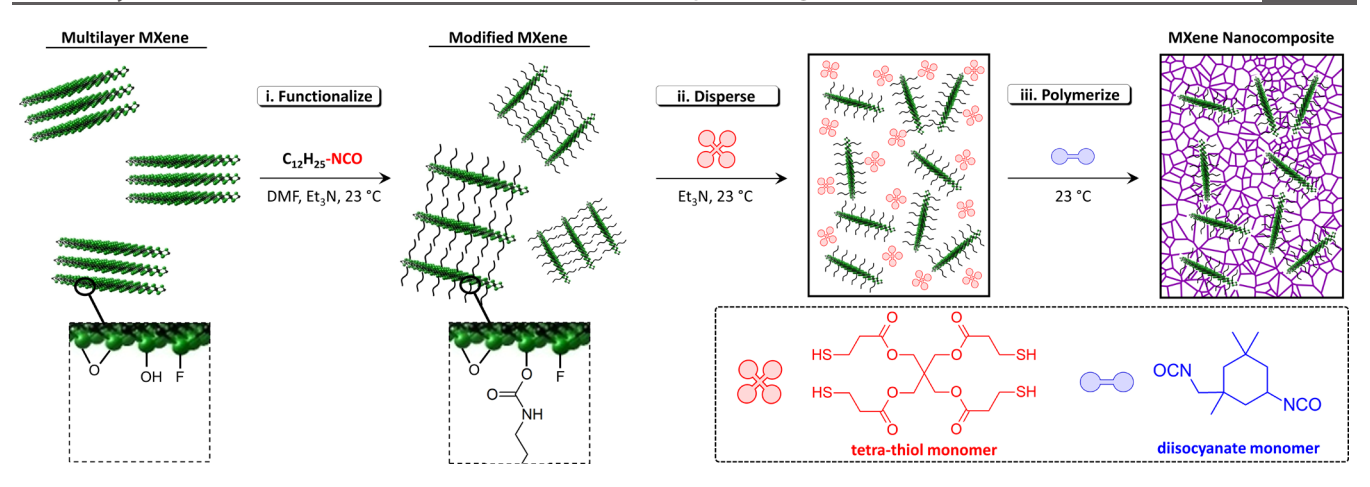


Figure 1. MXene thiourethane nanocomposites synthesized through (i) covalent functionalization and expansion of multilayer  $\text{Ti}_3C_2T_z$  through a reaction with dodecyl isocyanate, (ii) dispersion of modified  $\text{Ti}_3C_2T_z$  sheets within a tetrafunctional thiol monomer, and (iii) *in situ* polymerization and nanocomposite formation by the addition of a diisocyanate monomer under ambient conditions.

crylamide, 15 poly(vinyl alcohol), 16 and poly-(diallyldimethylammonium chloride). 16 However, film formation by aqueous filtration is challenging to scale up, wasteintensive, and limited to water-soluble thermoplastics. Moreover, MXenes can easily restack during filtration processes and differences in settling times can prevent the uniform distribution of filler throughout the film thickness. In addition, passage of a dissolved polymer through the filter creates difficulty in controlling filler loadings.<sup>17</sup> To address some of these limitations, several reports have instead utilized in situ polymerizations to prepare  $\stackrel{\circ}{\mathrm{MXene-polymer}}$  NCs.  $^{12,13,18-20}$  In such a process, the layered nanomaterial is typically intercalated with a monomer and then polymerization is initiated for composite formation. Advantageously, in situ polymerization has been shown to delaminate layered nanomaterials and facilitate uniform dispersion of nanosheets within polymer matrices. 18-21 Furthermore, unlike filtered NCs, in situ polymerization uniquely affords cross-linked polymer networks, enabling the synthesis of thermosetting and elastomeric MXene-polymer NCs.

It is well-recognized that the bulk properties of nanocomposites are highly dependent on the nanomaterial's dispersion.<sup>22</sup> The large surface area of nanomaterials provides improved nanocomposite properties at low loadings but simultaneously renders them prone to aggregation. 23,24 Aggregation has been identified as one of the greatest obstacles facing nanocomposite research regardless of the chosen nanomaterial or intended application. Recently, researchers have focused on the surface modification of MXenes<sup>18,19,27–52</sup> to improve their compatibility with solvents, monomers, and polymers, which has promise for facilitating the bulk synthesis of well-dispersed MXene-polymer NCs. Toward this goal, Ti<sub>3</sub>C<sub>2</sub>T<sub>z</sub> MXenes have been covalently modified by reacting -OH surface terminations with alkylsilanes, 32,34-36 alkylphosphonic acids, 31 carboxylic acids,<sup>29</sup> and isocyanates.<sup>28</sup> Chemical modification is a key step toward making MXenes useful as intercalated nanomaterials or fillers for polymer matrices; however, a scalable process for modifying MXenes has yet to be developed. Most studies on the chemical functionalization of  $\text{Ti}_3\text{C}_2\text{T}_z$  have been performed on *delaminated* MXenes,  $^{28-37,42-44,47-52}$  which are produced at relatively low yields using dilute suspensions (10-20 mg/mL) that hinder their industrial adoption.<sup>53</sup> In contrast,

the covalent surface modification of high-yielding *multilayer*  ${\rm Ti_3C_2T_z}$  has rarely been reported,  $^{27,38}$  and never with isocyanates, despite the wide scope of functional isocyanates that are commercially available. In this context, we view the modification of multilayers with isocyanates as an untapped synthetic platform to scalable quantities of surface-modified MXenes and well-dispersed MXene–polymer NCs for a variety of applications and advanced materials.

While surface modification is critical for well-dispersed nanocomposites and nanofiller compatibility, the underlying polymerization reaction must also be tolerant to the presence of filler and highly efficient to ensure proper network formation. Click chemistries, first described in 2001,<sup>54</sup> are a family of reactions that have been identified as a powerful and enabling tool for the synthesis of polymer materials because they are rapid, orthogonal, simple to perform, and proceed to quantitative conversions with few or little byproducts. 55-61 The thiol-isocyanate "click" reaction has proven to be particularly useful in polymer synthesis, offering flexibility and simplicity for polymer chain extensions, 62,63 chain-end modifications, 63,64 side group modifications, 65 and production of thiourethane polymer networks for encapsulation<sup>66</sup> and optical materials.<sup>67</sup> Thiourethane polymers produced via the thiol-isocyanate "click" reaction also share many desirable characteristics with the more common polyurethane (hydrogen bonding, elasticity, and impact resistance), with the additional advantages of adhering to many "click" chemistry attributes including extremely rapid reaction rates (comparable to amine-isocyanate reactions), high network uniformity, high monomer conversion, and few or no byproducts produced by the reaction.<sup>68</sup> Uniquely, thiourethane bonds also exhibit dynamic/reversible character at elevated temperatures and show promise as a chemistry for fully reprocessable network polymers with limited impact on mechanical properties.<sup>69,70</sup> We envisioned that the thiol-isocyanate "click" reactions may provide a straightforward and robust route to synthesizing MXene-polymer nanocomposites at room temperature under ambient conditions.

Inspired by Ruoff and co-workers who exfoliated graphene oxide through an isocyanate treatment, <sup>71,72</sup> we devised a powerful new strategy of synthesizing well-dispersed MXene–polymer NCs *via* (a) covalent modification of multilayer MXenes using functional isocyanates and (b) subsequent

dispersion of the modified MXene in monomers followed by their polymerization into a cross-linked polymer network (Figure 1). Specifically, in our approach, hydroxyl terminations on the surface of multilayer Ti<sub>3</sub>C<sub>2</sub>T<sub>z</sub> were reacted with dodecyl isocyanate to form an alkyl carbamate surface-functionalized MXene under mild conditions, as depicted in Figure 1 (step i). These modified MXenes were dispersed in a tetrafunctional thiol monomer and were then combined with a complementary difunctional isocyanate to initiate step-growth polymerization and NC formation (Figure 1, steps ii-iii). We designed our synthesis to use the thiol-isocyanate reaction for network formation because of its simple, robust, and rapid nature, which affords the convenience of in situ polymerization under fully ambient conditions (i.e., in air and at room temperature). Furthermore, our approach uniquely targets the utilization of higher-yielding, multilayer MXenes, contrary to significantly lower-yielding, delaminated MXene suspensions, enabling the production of well-dispersed MXene-polymer NCs in a more pragmatic and scalable manner. To the best of our knowledge, this contribution represents the first report of covalent modification to multilayer MXenes using isocyanates, as well as the first reported use of isocyanate-modified MXenes in a polymer NC.

# ■ RESULTS AND DISCUSSION

In the first step of our NC synthesis, we attempted to functionalize multilayer  $Ti_3C_2T_z$  through its hydroxyl terminations using an isocyanate treatment (Figure 1, step i). We reasoned, from successes with other nanofillers, that a covalent (nonpolar) surface modification to hydrophilic MXenes would aid in dispersing these 2D nanomaterials within hydrophobic polymer matrices. Toward this goal, multilayer  $Ti_3C_2T_z$  was stirred at room temperature in dimethylformamide (DMF) containing dodecyl isocyanate ( $C_{12}H_{25}$ –NCO) and a triethylamine catalyst ( $Et_3N$ ) for 24 h, which was then filtered and thoroughly washed to yield a light-gray powder. To gain insight into whether the isocyanate treatment caused any structural changes, X-ray diffraction (XRD) patterns of the dried MXene product were compared to that of the precursor multilayer  $Ti_3C_2T_z$  and parent MAX phase (Figure 2). The

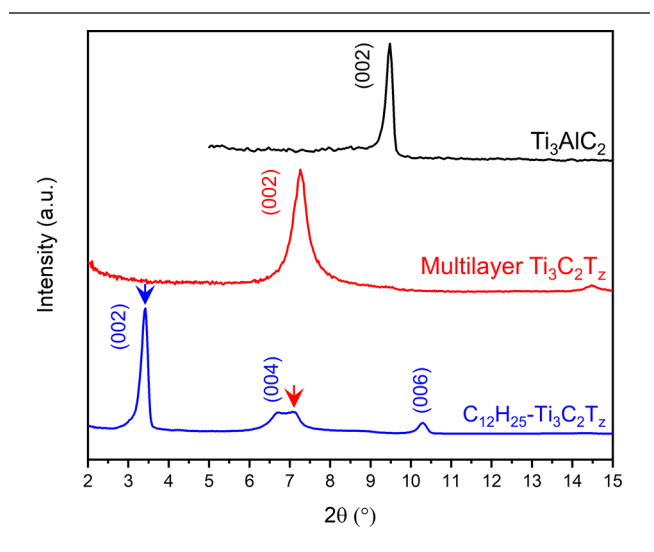


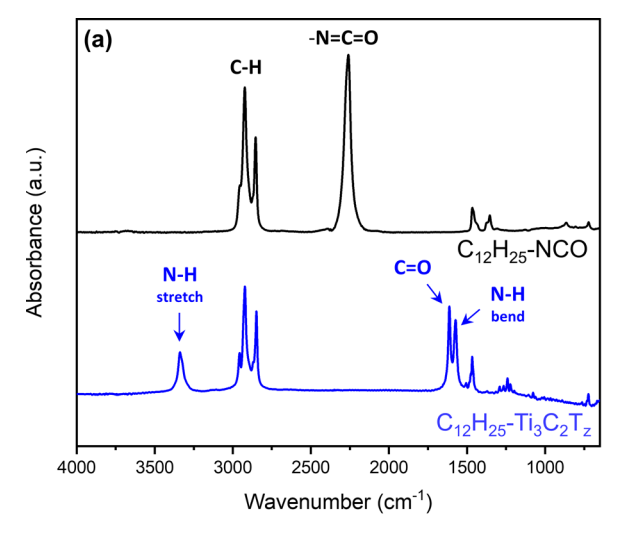
**Figure 2.** XRD patterns of the parent  $Ti_3AlC_2$  MAX phase (black), multilayer  $Ti_3C_2T_z$  MXene (red), and modified  $C_{12}H_{25}-Ti_3C_2T_z$  multilayer MXene (blue) after isocyanate treatment.

average spacing between MXene layers was determined through analysis of the 00l diffraction peak position, which is frequently used as an indicator of successful etching, intercalation, hydration, or dispersion of MXenes. <sup>18,75,76</sup> Beginning from the parent MAX phase, the 002 peak position shifted from a  $2\theta$  value of 9.48 to 7.26° after etching into multilayer  ${\rm Ti}_3{\rm C}_2{\rm T}_z$  using 10 wt % HF. This shift corresponds to a change in distance between the sheets  $(d_{002})$  from 9.3 to 12.2 Å, as Al layers were replaced with  $-{\rm O}$ ,  $-{\rm OH}$ , and/or  $-{\rm F}$  terminations. <sup>1,75</sup>

With multilayer MXene in hand, the isocyanate treatment was next performed. The treatment resulted in an even greater shift in the 002 peak position from 7.26 to 3.42°, yielding a final  $d_{002}$  of 25.8 Å. These data provide strong evidence for the successful intercalation of C<sub>12</sub>H<sub>25</sub>-NCO between the multilayer sheets. The large expansion of the intergallery spacing,  $d_{002}$ , was stable despite thorough washing with dichloromethane and hexanes, suggesting that covalent modification may have occurred. Our observed change in  $d_{002}$  aligns with results of Ghidiu et al., who demonstrated that multilayers intercalated with structurally similar functionalities (dodecyland hexadecyl-trimethylammonium cations) increased  $d_{002}$  to 18.9 Å (4.67°) and 38.0 Å (2.33°), respectively. The XRD also revealed a bimodal peak at  $\sim$ 7° in the  $\rm C_{12}H_{25}$ – $\rm Ti_3C_2T_z$ pattern, which we determined to be an overlap between the 004 reflection of  $C_{12}H_{25}$  –  $Ti_3C_2T_z$  and the 002 reflection of the unmodified multilayer Ti<sub>3</sub>C<sub>2</sub>T<sub>z</sub>. Deconvolution confirmed that the majority of multilayer  $Ti_3C_2T_z$  was converted to  $C_{12}H_{25}$ -Ti<sub>3</sub>C<sub>2</sub>T<sub>z</sub> using the relative intensities of the 002 reflections within the final product pattern  $(C_{12}H_{25}-Ti_3C_2T_z)$  (blue arrow)/ $Ti_3C_2T_z$  (red arrow)  $\approx 7$ ). See Figure S1 for intensities and deconvolution. Moreover, assignment of the 004 reflection within the bimodal peak was corroborated by the locations of the harmonics at 3.42° and 10.3° corresponding to the 002 and 006 reflections of the  $C_{12}H_{25}-Ti_3C_2T_z$ , respectively.

While XRD provided indirect support that our isocyanate treatment was successful, we sought to obtain direct structural evidence for the surface modification through Fourier transform infrared (FTIR) spectroscopy and nuclear magnetic resonance (NMR). FTIR analysis showed that the isocyanate treatment of MXene indeed exhibited key chemical signatures supporting carbamate (urethane) formation and covalent modification (Figure 3a). After purification of our isocyanate-treated MXene, a secondary amide stretching vibration (N-H), an important structural motif of the carbamate product, was now present in the  $C_{12}H_{25}-Ti_3C_2T_z$  spectrum at 3338 cm<sup>-1.77-80</sup> The carbamate linkage was further supported by the appearance of two additional signals arising from the carbonyl stretch (C=O) at 1613 cm<sup>-1</sup> and the secondary amide bend (N-H) at 1573 cm<sup>-1</sup> in the  $C_{12}H_{25}$ -Ti<sub>3</sub> $C_2T_z$ product.<sup>77,81</sup> Moreover, after purification, signals associated with the C-H stretching mode of the aliphatic chain (originating from the C<sub>12</sub>H<sub>25</sub>-NCO reactant) were now clearly visible in the spectrum of the modified multilayer at 2850, 2923, and 2955 cm<sup>-1</sup>. For reference, a spectrum of unmodified multilayer MXene is available in the Supporting Information (Figure S2).

To bolster the FTIR results,  $^1H$  NMR spectra were also obtained for the  $C_{12}H_{25}$ –NCO reactant and modified  $C_{12}H_{25}$ – $Ti_3C_2T_z$  product (Figure 3b). Resonances associated with the methylene protons adjacent to the isocyanate remained in the product (after purification) but shifted upfield following MXene modification (protons "a":  $3.29 \rightarrow 3.15$  ppm;



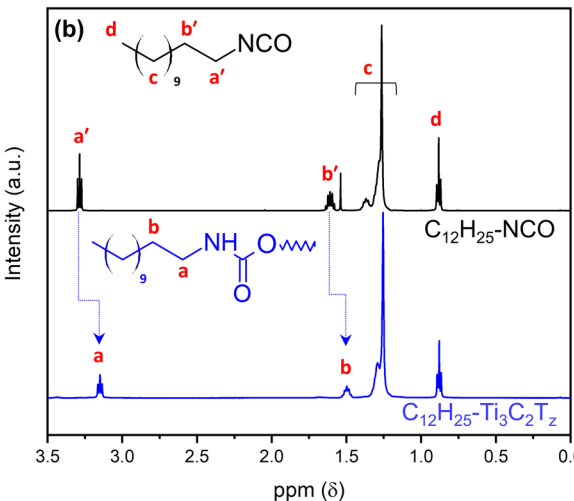


**Figure 3.** (a) FTIR and (b) NMR spectra of reactant  $C_{12}H_{25}$ –NCO and modified  $C_{12}H_{25}$ –Ti $_3C_2T_z$  after purification. Inset chemical structures represent reagent  $C_{12}H_{25}$ –NCO and the product alkyl carbamate (urethane) after modification.

protons "b":  $1.61 \rightarrow 1.50$  ppm). These chemical shifts provide evidence that a reaction took place and that nuclei "a" and "b" had entered a more shielded environment, likely from their close proximity to a more electron-rich carbamate and large, electropositive Ti atom (relative to an isocyanate). This upfield shift of the methylene protons "a" and "b" was also consistent with NMR predictive software. As expected, alkyl groups of greater distance from the reaction site showed essentially no change in chemical shift ("d" at 0.88 ppm and "c" at 1.25 ppm). Moreover, after purification, the C<sub>12</sub>H<sub>25</sub>-Ti<sub>3</sub>C<sub>2</sub>T<sub>z</sub> spectrum showed no evidence of the residual isocyanate reactant (b' and a'). <sup>1</sup>H NMR of unmodified MXene was not possible due to its poor solubility in chloroform. Taken collectively, the results from XRD, FTIR, and NMR provide strong evidence for intercalation and covalent functionalization of multilayer MXene using isocyanates, which to our knowledge, has never been reported in the literature.

To estimate the extent of functionalization, thermogravimetric analysis (TGA) was performed on the modified and unmodified multilayers (Figures 4 and S3). As anticipated, the unmodified  ${\rm Ti}_3{\rm C}_2{\rm T}_z$  multilayers showed a negligible change in mass up to 500 °C. In stark contrast, a significant mass loss was observed with the modified  ${\rm C}_{12}{\rm H}_{25}{\rm -Ti}_3{\rm C}_2{\rm T}_z$  between 160 and

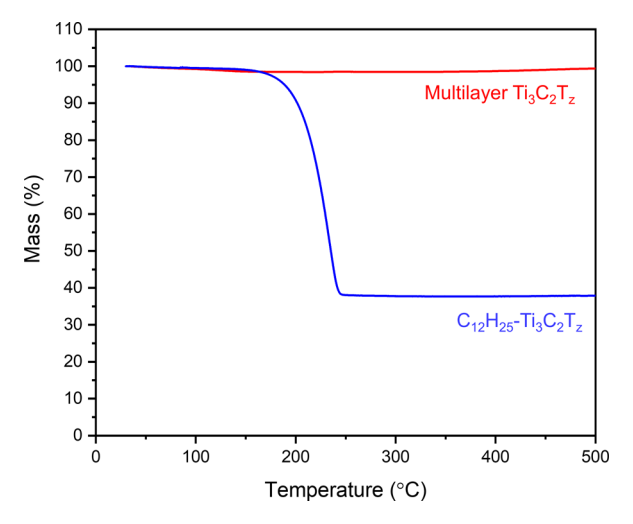


**Figure 4.** Percent mass vs temperature from TGA for multilayer  $Ti_3C_2T_z$  and modified  $C_{12}H_{25}-Ti_3C_2T_z$ .

250 °C, which we attribute to the decomposition of grafted alkyl chains on the MXene surfaces. Carbamates or urethane linkages are known to be reversible and to dissociate at temperatures exceeding 150 °C, 82 which in our case, would generate a rapidly lost decomposition product at the observed temperatures (e.g., boiling point of dodecyl isocyanate  $\approx$ 160 °C).

After complete decomposition, the residual MXene was determined to be ~38 wt %. Utilizing this value, we estimate that ~1.6 alkyl chains were attached to each MXene repeat unit (i.e.,  $[C_{12}H_{25}-NCO]/[Ti_3C_2T_z] \approx 1.55:1.00$ ), assuming z = 2 and that the  $Ti_3C_2T_z$  terminations were F/O/OH = 0.25/ 0.5/0.25, an energetically favorable composition described in computational studies. 83-85 Given that our approximation is reasonable, these calculations suggest that a stoichiometric ratio of surface grafts to MXene oxygen terminations exists (i.e.,  $[C_{12}H_{25}-NCO]/[T_{OH}+T_{O}] \approx 1.04:1.00$ ), implying that the oxygen-based terminations were quantitatively converted into alkyl carbamate surface functionalities (see the Supporting Information for detailed calculations). In other words, using our synthetic conditions, we surmise that the surface chemistry of Ti<sub>3</sub>C<sub>2</sub>T<sub>2</sub> is likely composed of ~75% reactive surface terminations (-OH and -O) and 25% unreactive surface terminations (-F). However, it should be noted that significant compositional variability exists in the literature concerning the surface terminations of HF-etched  ${\rm Ti}_3{\rm C}_2{\rm T}_{z}^{85-89}$  which would have minor implications on the aforementioned calculations. Regardless, we view our surface modification strategy with isocyanates as a highly efficient and versatile reaction platform for installing surface functionalities to MXenes, as well as a facile and quantitative means to approximate the concentration of oxygen-based terminations on Ti<sub>3</sub>C<sub>2</sub>T<sub>2</sub> and presumably other MXenes.

The unmodified and modified multilayers were next incorporated into a "click" curable thiourethane thermoset to assess differences in nanofiller dispersibility in a polymer matrix (Figure 1, steps ii–iii). In both cases, NCs were loaded to 5 wt % filler (unmodified Ti<sub>3</sub>C<sub>2</sub>T<sub>z</sub> or modified C<sub>12</sub>H<sub>25</sub>–Ti<sub>3</sub>C<sub>2</sub>T<sub>z</sub>). The NCs were prepared by first combining filler, tetrathiol, and Et<sub>3</sub>N catalyst, followed by homogenization on a planetary centrifugal mixer (step ii). Isophorone diisocyanate was then added to initiate polymerization, which was quickly followed by solidification (step iii). After annealing, dynamic mechanical

analysis revealed typical thermomechanical behavior for a thiourethane network, confirming the successful formation of MXene-polymer NCs (Figure 5). We observed that the

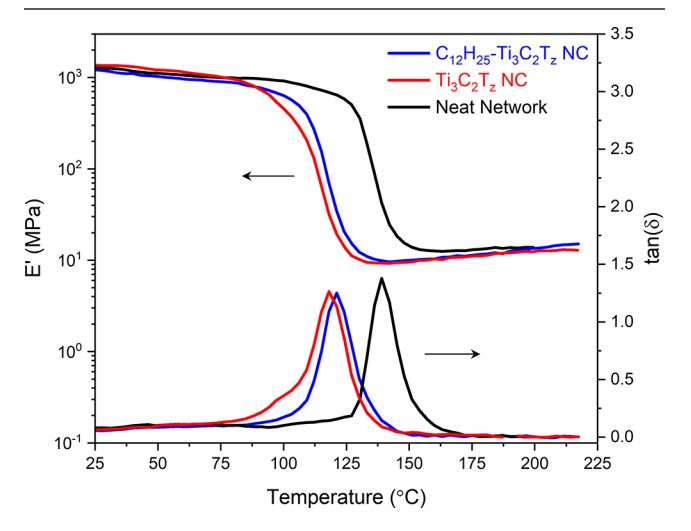


**Figure 5.** Storage modulus (E') and  $\tan(\delta)$  of thiourethane NCs using unmodified  $T_{i_3}C_2T_z$  and modified  $C_{12}H_{25}-T_{i_3}C_2T_z$  from dynamic mechanical analysis. A neat thiourethane network is shown for reference.

storage moduli (E') of both NCs were similar in magnitude to the literature <sup>69,90,91</sup> and that the  $\tan(\delta)$  peaks were consistently narrow (indicating the formation of uniform networks) also in alignment with the literature. <sup>91</sup>

Interestingly, NCs synthesized with modified and unmodified MXenes both displayed depressed  $T_{\rm g}$ 's, approximated at the max  $\tan(\delta)$ , compared to a thiourethane control (NCs:  $T_{\rm g} \approx 120~{\rm ^{\circ}C}$  vs neat network:  $T_{\rm g} \approx 139~{\rm ^{\circ}C}$ ). This reduction in  $T_{\rm g}$  may result from the nanofiller's nonpolar surface groups acting as a plasticizer (in the case of  $C_{12}H_{25}-Ti_3C_2T_z$ ) or from the generation of "softened" filler—matrix interfaces, which have depressed  $T_{\rm g}$  in other NCs. <sup>92–94</sup> While further research is required to develop an in-depth understanding of the impact of MXenes on  $T_{\rm g}$  and other NC properties (such research efforts are ongoing), the primary purpose of this contribution was to

develop and outline a facile and scalable method to produce well-dispersed MXene-polymer NCs.

After characterizing the thermomechanical behavior of the NCs, we sought to determine the influence of surface modification on nanofiller dispersion using XRD and scanning electron microscopy (SEM). Our analysis showed that a profound difference in filler dispersion existed between the NCs produced with unmodified and modified multilayers. As illustrated in Figure 6a, XRD of the modified MXene system revealed a nearly featureless pattern after polymerization into a nanocomposite (blue patterns,  $C_{12}H_{25}-Ti_3C_2T_2 \rightarrow C_{12}H_{25}-$ Ti<sub>3</sub>C<sub>2</sub>T<sub>z</sub> NC), resembling that of a thiourethane matrix without MXene (see Figure S4). Since no new low-angle peaks were observed, our XRD results indicate that the stacking of the MXene sheets was disrupted and that the majority of the modified Ti<sub>3</sub>C<sub>2</sub>T<sub>z</sub> was dispersed into the matrix. 95 In contrast, NCs produced with unmodified Ti<sub>3</sub>C<sub>2</sub>T<sub>z</sub> showed clear persistence of the basal peak at 7.26° with minimal change in position or intensity (red patterns, multilayer  ${\rm Ti_3C_2T_z} \rightarrow {\rm Ti_3C_2T_z}$  NC). This implies that the modification of Ti<sub>3</sub>C<sub>2</sub>T<sub>2</sub> with isocyanate and the resulting interlayer expansion were crucial for dispersing Ti<sub>3</sub>C<sub>2</sub>T<sub>2</sub> sheets in the polymer matrix. For reference, additional XRD patterns are available of the NCs with intensity values (Figure S5).

To complement XRD, SEM and energy-dispersive spectroscopy (EDS) were also performed on cross-sectional fracture surfaces of the NCs to further assess nanofiller dispersion (Figure 6b). Visually, EDS mapping for Ti confirmed that the MXene nanofiller was incorporated throughout both samples (magenta signal); however, its distribution was greatly impacted by the covalent modification. For comparison, we determined the number and size of MXene domains (referred to as particles) within each NC using the EDS results in conjunction with image analysis to quantify local, highconcentration clusters of the Ti signal. Our analysis revealed that the normalized particle count (per gram of  $Ti_3C_2T_z$ ) was reduced by fourfold for the modified NC compared to its unmodified counterpart (Table S1). Fewer clusters in the modified NC reinforce our XRD data and the notion that the nanofiller dispersion was improved by covalent modification before nanocomposite synthesis. This postulation of improved

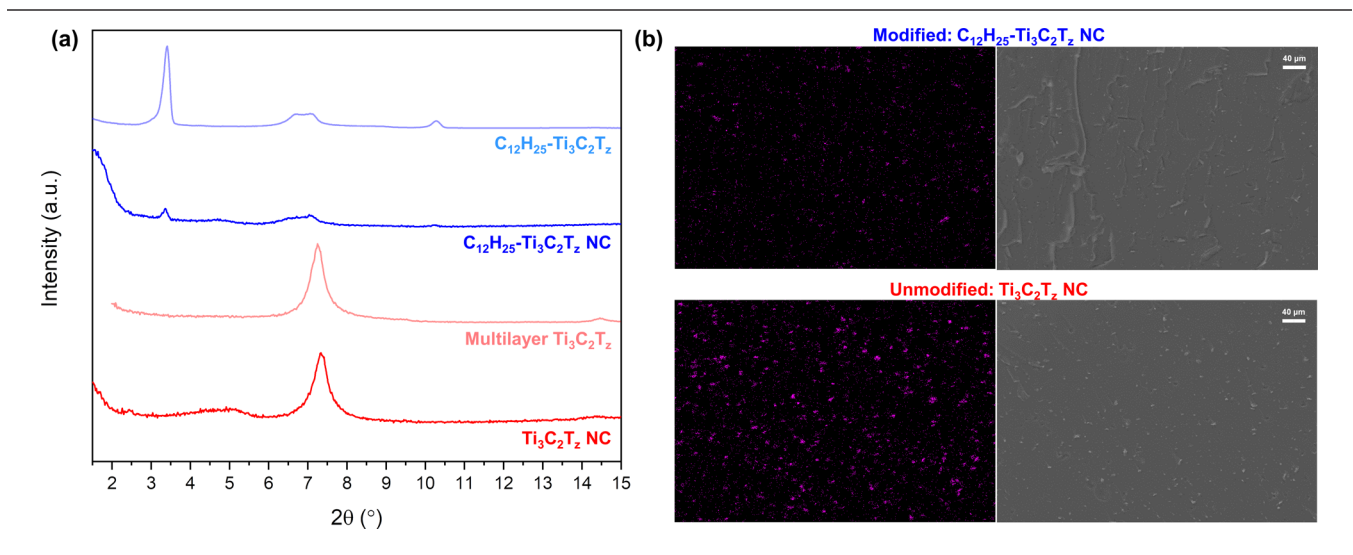


Figure 6. (a) Diffraction patterns of NCs synthesized using unmodified  $T_{13}C_2T_z$  and modified  $C_{12}H_{25}-T_{13}C_2T_z$ . (b) EDS maps of Ti (left) and the corresponding SEM images of fracture surfaces (right) of modified  $C_{12}H_{25}-T_{13}C_2T_z$ , NC (top) and unmodified  $T_{13}C_2T_z$ , NC (bottom).

dispersion was further supported by a comparison of fracture surfaces of the nanocomposites using SEM (Figure 6b). The fracture surface of the modified  $C_{12}H_{25}-Ti_3C_2T_z$  NC showed a distinct roughness as opposed to the smooth fracture surfaces of the unmodified NC and neat thiourethane without MXene (Figure S6). A rough fracture surface suggests that the nanofiller more frequently encountered the propagating crack front, which is consistent with better filler dispersion. 95–97

## CONCLUSIONS

Herein, for the first time, we demonstrate a straightforward method for covalent modification of multilayer MXene using isocyanates and demonstrate the utility of this synthetic approach for the facile production of well-dispersed MXenepolymer NCs under ambient conditions. Nanocomposites produced at 5 wt % filler using modified MXenes, compared to their unmodified counterparts, exhibited greatly enhanced nanofiller dispersion within a thiourethane network. Our results also reveal that the isocyanate treatment can be used as a tool to produce high grafting density surface modifications to MXenes and for the quantification of oxygen-based terminations on Ti<sub>3</sub>C<sub>2</sub>T<sub>z</sub>. We envision that our approach will serve as a powerful and versatile synthetic platform for the attachment of various functional moieties to MXene surfaces and for enabling the development of next-generation nanocomposites with fascinating new properties.

## EXPERIMENTAL SECTION

MAX Phase Synthesis. The  ${\rm Ti_3AlC_2}$  MAX phase was synthesized with TiC, Al, and Ti powders at a molar ratio of 2:1.05:1, respectively. The powders were ball-milled for 24 h, then transferred to an alumina  ${\rm (Al_2O_3)}$  boat, and heated in an  ${\rm Al_2O_3}$  tube furnace to 1350 °C with a heating rate of 5 °C/min under argon flow. After 2 h, the sample was cooled passively to room temperature. The resulting porous sintered brick was milled into a powder using a drill press. The resulting powder was passed through a 400 mesh sieve to ensure that only particle sizes <38  $\mu$ m were left.

MXene Synthesis. Multilayer Ti<sub>3</sub>C<sub>2</sub>T<sub>z</sub> was produced following methods described previously. In short, 1.08 g of lithium chloride (LiCl) was slowly added to a bottle containing 10 mL of 10 wt % hydrofluoric acid. Once the LiCl was fully dissolved, 1 g of Ti<sub>3</sub>AlC<sub>2</sub> powder was added to the solution and the mixture was left to stir at 300 rpm at room temperature for 24 h. After etching was complete, the solution was divided into two 50 mL centrifuge tubes—5 mL per tube—and centrifuged at 3500 rpm for 60 s. The supernatant was decanted and replaced with 40 mL of deionized (DI) water. The tubes were each vortexed for 30 s to redisperse the sediment and were then again centrifuged for 3500 rpm for 60 s. This process was repeated until a pH of 6, as measured by pH paper, was reached. After washing, the sediment was redispersed in 20 mL of DI water and was filtered onto a polypropylene membrane and then was dried in a vacuum oven at 100 °C for 12 h.

**Modification of MXenes with C**<sub>12</sub>H<sub>25</sub>–**NCO.** The modification of  $Ti_3C_2T_z$  with  $C_{12}H_{25}$ –**NCO** was performed as follows: The experiment was formulated assuming an equal concentration of –OH, –O, and –F terminations on  $Ti_3C_2T_z$  and using a molar ratio of  $[C_{12}H_{25}$ –**NCO**]/[-OH] = 10/1. Therefore, 0.125 g of multilayer  $Ti_3C_2T_z$ , 0.03 mmol Et<sub>3</sub>N, and 4.72 g of dried DMF were first added to a 50 mL round-bottom flask containing a magnetic stir bar. The sealed round-bottom flask was subsequently placed in an ultrasonication bath and sonicated and sparged with N<sub>2</sub> gas for 1 h. Using a syringe,  $C_{12}H_{25}$ –**NCO** was added to the round-bottom flask in a dropwise fashion. The round-bottom flask was immediately transferred to a stir plate and the reaction mixture was allowed to stir at room temperature for 24 h. The suspension was then transferred to a vacuum filtration setup and was filtered and thoroughly washed using

60 mL of dichloromethane followed by 60 mL of hexanes. The resulting film was dried in a vacuum oven at 23  $^{\circ}$ C overnight.

**Nanocomposite Synthesis.** Neat and nanocomposite samples were produced as follows: Nanocomposite samples were formulated with 5 wt % filler  $(Ti_3C_2T_z \text{ or } C_{12}H_{25}-Ti_3C_2T_z \text{ with respect to monomer})$  and at an equimolar ratio of thiol and isocyanate groups for the polymer matrix ([SH]/[NCO] = 1). Dried  $Ti_3C_2T_z$  or  $C_{12}H_{25}-Ti_3C_2T_z$  powder, TEA (0.125 mol % catalyst for composite samples and 0.025 mol % for neat samples), and pentaerythritol tetrakis(3-mercaptopropionate) were added to a 20 mL scintillation vial. The scintillation vial was mixed on a planetary centrifugal mixer (ARE-310, THINKY) at 2000 rpm for 5 min. Once the solution was homogenized, isophorone diisocyanate was added to the vial using a syringe. The solution was agitated using a vortex mixer for 10 s and was subsequently cast into a silicone tensile mold. Samples were allowed to rest in the mold for 1 h and then were annealed for 24 h at 90 °C.

## ASSOCIATED CONTENT

# Supporting Information

The Supporting Information is available free of charge at https://pubs.acs.org/doi/10.1021/acs.chemmater.0c03972.

Reagents, instruments, methods, analysis, and references; XRD of modified multilayer  $(C_{12}H_{25}-Ti_3C_2T_z)$ with intensity values and deconvolution; FTIR spectrum of multilayer Ti<sub>3</sub>C<sub>2</sub>T<sub>z</sub> powder without isocyanate treatment; derivative of the  $C_{12}H_{25}-Ti_3C_2T_z$  mass loss curve vs temperature from TGA for the identification of onset, peak, and final degradation temperatures; XRD of a neat thiourethane network without MXene filler and modified C<sub>12</sub>H<sub>25</sub>-Ti<sub>3</sub>C<sub>2</sub>T<sub>2</sub> nanocomposite; XRD patterns showing relative intensities of modified C<sub>12</sub>H<sub>25</sub>- $Ti_3C_2T_z$  and nanocomposite, and unmodified  $Ti_3C_2T_z$ and nanocomposite; SEM image of the control sample fracture surface and EDS mapping for titanium; and nanocomposite results from Imagel analysis using EDS maps with particle count, normalized particle count, and particle size (PDF)

# AUTHOR INFORMATION

# **Corresponding Author**

Andrew J. D. Magenau — Department of Materials Science and Engineering, Drexel University, Philadelphia, Pennsylvania 19104, United States; oorcid.org/0000-0002-7565-9075; Email: ajm496@drexel.edu

### **Authors**

Riki M. McDaniel – Department of Materials Science and Engineering, Drexel University, Philadelphia, Pennsylvania 19104, United States

Michael S. Carey – Department of Materials Science and Engineering, Drexel University, Philadelphia, Pennsylvania 19104. United States

Olivia R. Wilson – Department of Materials Science and Engineering, Drexel University, Philadelphia, Pennsylvania 19104, United States

Michel W. Barsoum – Department of Materials Science and Engineering, Drexel University, Philadelphia, Pennsylvania 19104, United States; © orcid.org/0000-0001-7800-3517

Complete contact information is available at: https://pubs.acs.org/10.1021/acs.chemmater.0c03972

# Notes

The authors declare no competing financial interest.

# ACKNOWLEDGMENTS

A.J.D.M. would like to thank the ACS Petroleum Research Fund (59903-DNI7) and the Pennsylvania Manufacturing Innovation Program for partial support of this research. M.W.B. would like to thank the Division of Materials Research of the National Science Foundation (DMR 1740795) for support of this research. The authors also thank David Howe and Varun Natu for their helpful discussions and commentary, and Patricia Lyons of Moorestown NJ for her artistic help with the cover art. The authors acknowledge Dr. Giuseppe Palmese and Zachary Hinton for their support and for use of laboratory equipment. MarvinSketch is gratefully acknowledged for generous allowance of an academic license for this work.

## REFERENCES

- (1) Naguib, M.; Mashtalir, O.; Carle, J.; Presser, V.; Lu, J.; Hultman, L.; Gogotsi, Y.; Barsoum, M. W. Two-Dimensional Transition Metal Carbides. *ACS Nano* **2012**, *6*, 1322–1331.
- (2) Naguib, M.; Kurtoglu, M.; Presser, V.; Lu, J.; Niu, J.; Heon, M.; Hultman, L.; Gogotsi, Y.; Barsoum, M. W. Two-dimensional nanocrystals produced by exfoliation of Ti<sub>3</sub>AlC<sub>2</sub>. *Adv. Mater.* **2011**, 23, 4248–4253.
- (3) Shahzad, F.; Alhabeb, M.; Hatter, C. B.; Anasori, B.; Man Hong, S.; Koo, C. M.; Gogotsi, Y. Electromagnetic interference shielding with 2D transition metal carbides (MXenes). *Science* **2016**, *353*, 1137–1140.
- (4) Natu, V.; Clites, M.; Pomerantseva, E.; Barsoum, M. W. Mesoporous MXene powders synthesized by acid induced crumpling and their use as Na-ion battery anodes. *Mater. Res. Lett.* **2018**, *6*, 230–235.
- (5) Hantanasirisakul, K.; Zhao, M.-Q.; Urbankowski, P.; Halim, J.; Anasori, B.; Kota, S.; Ren, C. E.; Barsoum, M. W.; Gogotsi, Y. Fabrication of  ${\rm Ti}_3{\rm C}_2{\rm T}_{\rm x}$  MXene Transparent Thin Films with Tunable Optoelectronic Properties. *Adv. Bioelectron. Mater.* **2016**, *2*, 1600050.
- (6) Chia, X.; Pumera, M. Characteristics and performance of two-dimensional materials for electrocatalysis. *Nat. Catal.* **2018**, *1*, 909–921.
- (7) Huang, K.; Li, Z.; Lin, J.; Han, G.; Huang, P. Two-dimensional transition metal carbides and nitrides (MXenes) for biomedical applications. *Chem. Soc. Rev.* **2018**, *47*, 5109–5124.
- (8) Zhang, H.; Wang, L.; Chen, Q.; Li, P.; Zhou, A.; Cao, X.; Hu, Q. Preparation, mechanical and anti-friction performance of MXene/polymer composites. *Mater. Des.* **2016**, *92*, *682*–*689*.
- (9) An, H.; Habib, T.; Shah, S.; Gao, H.; Radovic, M.; Green, M. J.; Lutkenhaus, J. L. Surface-agnostic highly stretchable and bendable conductive MXene multilayers. *Sci. Adv.* **2018**, *4*, No. eaaq0118.
- (10) Mayerberger, E. A.; Urbanek, O.; McDaniel, R. M.; Street, R. M.; Barsoum, M. W.; Schauer, C. L. Preparation and characterization of polymer- $Ti_3C_2T_x$  (MXene) composite nanofibers produced via electrospinning. *J. Appl. Polym. Sci.* **2017**, *134*, 45295.
- (11) Zhang, Y.-Z.; Lee, K. H.; Anjum, D. H.; Sougrat, R.; Jiang, Q.; Kim, H.; Alshareef, H. N. MXenes stretch hydrogel sensor performance to new limits. *Sci. Adv.* **2018**, *4*, No. eaat0098.
- (12) Boota, M.; Anasori, B.; Voigt, C.; Zhao, M.-Q.; Barsoum, M. W.; Gogotsi, Y. Pseudocapacitive Electrodes Produced by Oxidant-Free Polymerization of Pyrrole between the Layers of 2D Titanium Carbide (MXene). *Adv. Mater.* **2016**, 28, 1517–1522.
- (13) Chen, C.; Boota, M.; Xie, X.; Zhao, M.; Anasori, B.; Ren, C. E.; Miao, L.; Jiang, J.; Gogotsi, Y. Charge transfer induced polymerization of EDOT confined between 2D titanium carbide layers. *J. Mater. Chem. A* **2017**, *5*, 5260–5265.
- (14) Li, K.; Wang, X.; Li, S.; Urbankowski, P.; Li, J.; Xu, Y.; Gogotsi, Y. An Ultrafast Conducting Polymer@MXene Positive Electrode with High Volumetric Capacitance for Advanced Asymmetric Supercapacitors. *Small* **2019**, *16*, 1906851.
- (15) Naguib, M.; Saito, T.; Lai, S.; Rager, M. S.; Aytug, T.; Parans Paranthaman, M.; Zhao, M.-Q.; Gogotsi, Y. Ti<sub>3</sub>C<sub>2</sub>T<sub>x</sub> (MXene)—

- polyacrylamide nanocomposite films. RSC Adv. 2016, 6, 72069-72073.
- (16) Ling, Z.; Ren, C. E.; Zhao, M.-Q.; Yang, J.; Giammarco, J. M.; Qiu, J.; Barsoum, M. W.; Gogotsi, Y. Flexible and conductive MXene films and nanocomposites with high capacitance. *Proc. Natl. Acad. Sci. U. S. A* **2014**, *111*, 16676–16681.
- (17) Gao, L.; Li, C.; Huang, W.; Mei, S.; Lin, H.; Ou, Q.; Zhang, Y.; Guo, J.; Zhang, F.; Xu, S.; Zhang, H. MXene/Polymer Membranes: Synthesis, Properties, and Emerging Applications. *Chem. Mater.* **2020**, 32, 1703–1747.
- (18) Carey, M.; Hinton, Z.; Sokol, M.; Alvarez, N. J.; Barsoum, M. W. Nylon- $6/\text{Ti}_3\text{C}_2\text{T}_z$  MXene Nanocomposites Synthesized by in Situ Ring Opening Polymerization of  $\varepsilon$ -Caprolactam and Their Water Transport Properties. *ACS Appl. Mater. Interfaces* **2019**, *11*, 20425–20436.
- (19) Carey, M. S.; Sokol, M.; Palmese, G. R.; Barsoum, M. W. Water Transport and Thermomechanical Properties of  $Ti_3C_2T_z$  MXene Epoxy Nanocomposites. *ACS Appl. Mater. Interfaces* **2019**, *11*, 39143–39149.
- (20) Carey, M.; Hinton, Z.; Natu, V.; Pai, R.; Sokol, M.; Alvarez, N. J.; Kalra, V.; Barsoum, M. W. Dispersion and Stabilization of Alkylated Ti<sub>3</sub>C<sub>2</sub>T<sub>z</sub> MXene in Nonpolar Solvents. *Cell Reports Physical Science* **2020**, *1*, 100042.
- (21) Potts, J. R.; Dreyer, D. R.; Bielawski, C. W.; Ruoff, R. S. Graphene-based polymer nanocomposites. *Polymer* **2011**, *52*, 5–25.
- (22) Ajayan, P. M.; Schadler, L. S.; Braun, P. V. Nanocomposite Science and Technology; John Wiley & Sons, 2006; pp 77–154.
- (23) Khare, H. S.; Burris, D. L. A quantitative method for measuring nanocomposite dispersion. *Polymer* **2010**, *51*, 719–729.
- (24) Fiedler, B.; Gojny, F. H.; Wichmann, M. H. G.; Nolte, M. C. M.; Schulte, K. Fundamental aspects of nano-reinforced composites. *Compos. Sci. Technol.* **2006**, *66*, 3115–3125.
- (25) Ke, Y.; Stroeve, P. Polymer-Layered Silicate and Silica Nanocomposites; Elsevier, 2005; pp 69–118.
- (26) Müller, K.; Bugnicourt, E.; Latorre, M.; Jorda, M.; Echegoyen Sanz, Y.; Lagaron, J.; Miesbauer, O.; Bianchin, A.; Hankin, S.; Bölz, U.; Pérez, G.; Jesdinszki, M.; Lindner, M.; Scheuerer, Z.; Castelló, S.; Schmid, M. Review on the Processing and Properties of Polymer Nanocomposites and Nanocoatings and Their Applications in the Packaging, Automotive and Solar Energy Fields. *Nanomaterials* **2017**, 7–74
- (27) Cao, W.-T.; Feng, W.; Jiang, Y.-Y.; Ma, C.; Zhou, Z.-F.; Ma, M.-G.; Chen, Y.; Chen, F. Two-dimensional MXene-reinforced robust surface superhydrophobicity with self-cleaning and photothermal-actuating binary effects. *Mater. Horiz.* **2019**, *6*, 1057–1065.
- (28) Bian, R.; Xiang, S.; Cai, D. Fast Treatment of MXene Films with Isocyanate to Give Enhanced Stability. *ChemNanoMat* **2019**, *6*, 64–67.
- (29) Guo, Q.; Zhang, X.; Zhao, F.; Song, Q.; Su, G.; Tan, Y.; Tao, Q.; Zhou, T.; Yu, Y.; Zhou, Z.; Lu, C. Protein-Inspired Self-Healable Ti<sub>3</sub>C<sub>2</sub> MXenes/Rubber-Based Supramolecular Elastomer for Intelligent Sensing. *ACS Nano* **2020**, *14*, 2788–2797.
- (30) Hao, L.; Zhang, H.; Wu, X.; Zhang, J.; Wang, J.; Li, Y. Novel thin-film nanocomposite membranes filled with multi-functional Ti<sub>3</sub>C<sub>2</sub>T<sub>x</sub> nanosheets for task-specific solvent transport. *Composites, Part A* **2017**, *100*, 139–149.
- (31) Kim, D.; Ko, T. Y.; Kim, H.; Lee, G. H.; Cho, S.; Koo, C. M. Nonpolar Organic Dispersion of 2D  $\mathrm{Ti_3C_2T_x}$  MXene Flakes via Simultaneous Interfacial Chemical Grafting and Phase Transfer Method. *ACS Nano* **2019**, *13*, 13818–13828.
- (32) Kumar, S.; Lei, Y.; Alshareef, N. H.; Quevedo-Lopez, M. A.; Salama, K. N. Biofunctionalized two-dimensional Ti<sub>3</sub>C<sub>2</sub> MXenes for ultrasensitive detection of cancer biomarker. *Biosens. Bioelectron.* **2018**, 121, 243–249.
- (33) Lim, S.; Park, H.; Yang, J.; Kwak, C.; Lee, J. Stable colloidal dispersion of octylated Ti<sub>3</sub>C<sub>2</sub>-MXenes in a nonpolar solvent. *Colloids Surf., A* **2019**, 579, 123648.
- (34) Riazi, H.; Anayee, M.; Hantanasirisakul, K.; Shamsabadi, A. A.; Anasori, B.; Gogotsi, Y.; Soroush, M. Surface Modification of a

- MXene by an Aminosilane Coupling Agent. Adv. Mater. Interfaces 2020, 7, 1902008.
- (35) Zhang, J.; Liu, Y.; Lv, Z.; Zhao, T.; Li, P.; Sun, Y.; Wang, J. Sulfonated  $\mathrm{Ti_3C_2T_x}$  to construct proton transfer pathways in polymer electrolyte membrane for enhanced conduction. *Solid State Ionics* **2017**, *310*, 100–111.
- (36) Zhao, J.; Yang, Y.; Yang, C.; Tian, Y.; Han, Y.; Liu, J.; Yin, X.; Que, W. A hydrophobic surface enabled salt-blocking 2D Ti<sub>3</sub>C<sub>2</sub> MXene membrane for efficient and stable solar desalination. *J. Mater. Chem. A* **2018**, *6*, 16196–16204.
- (37) Lei, Y.; Cui, Y.; Huang, Q.; Dou, J.; Gan, D.; Deng, F.; Liu, M.; Li, X.; Zhang, X.; Wei, Y. Facile preparation of sulfonic groups functionalized Mxenes for efficient removal of methylene blue. *Ceram. Int.* **2019**, *45*, 17653–17661.
- (38) Wang, H.; Zhang, J.; Wu, Y.; Huang, H.; Li, G.; Zhang, X.; Wang, Z. Surface modified MXene Ti3C2 multilayers by aryl diazonium salts leading to large-scale delamination. *Appl. Surf. Sci.* **2016**, 384, 287–293.
- (39) Carey, M.; Hinton, Z.; Natu, V.; Pai, R.; Sokol, M.; Alvarez, N. J.; Kalra, V.; Barsoum, M. W. Dispersion and Stabilization of Alkylated 2D MXene in Nonpolar Solvents and Their Pseudocapacitive Behavior. *Cell Rep. Phys. Sci.* **2020**, *1*, 100042.
- (40) Chen, J.; Chen, K.; Tong, D.; Huang, Y.; Zhang, J.; Xue, J.; Huang, Q.; Chen, T. CO<sub>2</sub> and temperature dual responsive "Smart" MXene phases. *Chem. Commun.* **2015**, *51*, 314–317.
- (41) He, L.; Wang, J.; Wang, B.; Wang, X.; Zhou, X.; Cai, W.; Mu, X.; Hou, Y.; Hu, Y.; Song, L. Large-scale production of simultaneously exfoliated and Functionalized Mxenes as promising flame retardant for polyurethane. *Composites, Part B* **2019**, *179*, 107486.
- (42) Sheng, X.; Zhao, Y.; Zhang, L.; Lu, X. Properties of two-dimensional Ti<sub>3</sub>C<sub>2</sub> MXene/thermoplastic polyurethane nanocomposites with effective reinforcement via melt blending. *Compos. Sci. Technol.* **2019**, *181*, 107710.
- (43) Si, J.-Y.; Tawiah, B.; Sun, W.-L.; Lin, B.; Wang, C.; Yuen, A.; Yu, B.; Li, A.; Yang, W.; Lu, H.-D.; Chan, Q.; Yeoh, G. Functionalization of MXene Nanosheets for Polystyrene towards High Thermal Stability and Flame Retardant Properties. *Polymers* 2019, 11, 976.
- (44) Taloub, N.; Henniche, A.; Liu, L.; Li, J.; Rahoui, N.; Hegazy, M.; Huang, Y. Improving the mechanical properties, UV and hydrothermal aging resistance of PIPD fiber using MXene (Ti<sub>3</sub>C<sub>2</sub>(OH)<sub>2</sub>) nanosheets. *Composites, Part B* **2019**, *163*, 260–271.
- (45) Tran, M. H.; Brilmayer, R.; Liu, L.; Zhuang, H.; Hess, C.; Andrieu-Brunsen, A.; Birkel, C. S. Synthesis of a Smart Hybrid MXene with Switchable Conductivity for Temperature Sensing. ACS Appl. Nano Mater. 2020, 3, 4069–4076.
- (46) Wei, L.; Wang, J.-W.; Gao, X.-H.; Wang, H.-Q.; Wang, X.-Z.; Ren, H. Enhanced Dielectric Properties of a Poly(dimethyl siloxane) Bimodal Network Percolative Composite with MXene. *ACS Appl. Mater. Interfaces* **2020**, *12*, 16805–16814.
- (47) Boota, M.; Urbankowski, P.; Porzio, W.; Barba, L.; Osti, N. C.; Bleuel, M.; Keum, J. K.; Mamontov, E. Understanding Functionalization of Titanium Carbide (MXene) with Quinones and Their Pseudocapacitance. ACS Appl. Energy Mater. 2020, 3, 4127.
- (48) Chen, K.; Yan, X.; Li, J.; Jiao, T.; Cai, C.; Zou, G.; Wang, R.; Wang, M.; Zhang, L.; Peng, Q. Preparation of Self-Assembled Composite Films Constructed by Chemically-Modified MXene and Dyes with Surface-Enhanced Raman Scattering Characterization. *Nanomaterials* **2019**, *9*, 284.
- (49) Derradji, M.; Trache, D.; Henniche, A.; Zegaoui, A.; Medjahed, A.; Tarchoun, A. F.; Belgacemi, R. On the preparation and properties investigations of highly performant MXene (Ti<sub>3</sub>C<sub>2</sub>(OH)<sub>2</sub>) nanosheets-reinforced phthalonitrile nanocomposites. *Adv. Compos. Lett.* **2019**, 28, 2633366X19890621.
- (50) Ji, J.; Zhao, L.; Shen, Y.; Liu, S.; Zhang, Y. Covalent stabilization and functionalization of MXene via silylation reactions with improved surface properties. *FlatChem* **2019**, *17*, 100128.

- (51) Shao, J.; Wang, J.-W.; Liu, D.-N.; Wei, L.; Wu, S.-Q.; Ren, H. A novel high permittivity percolative composite with modified MXene. *Polymer* **2019**. *174*, 86–95.
- (52) Chen, K.; Chen, Y.; Deng, Q.; Jeong, S.-H.; Jang, T.-S.; Du, S.; Kim, H.-E.; Huang, Q.; Han, C.-M. Strong and biocompatible poly(lactic acid) membrane enhanced by Ti<sub>3</sub>C<sub>2</sub>T<sub>z</sub> (MXene) nanosheets for Guided bone regeneration. *Mater. Lett.* **2018**, 229, 114–117.
- (53) Verger, L.; Natu, V.; Carey, M.; Barsoum, M. W. MXenes: An Introduction of Their Synthesis, Select Properties, and Applications. *Trends Chem.* **2019**, *1*, 656–669.
- (54) Kolb, H. C.; Finn, M. G.; Sharpless, K. B. Click Chemistry: Diverse Chemical Function from a Few Good Reactions. *Angew. Chem., Int. Ed.* **2001**, 40, 2004–2021.
- (55) Binder, W. H.; Sachsenhofer, R. "Click" Chemistry in Polymer and Materials Science. *Macromol. Rapid Commun.* **2007**, 28, 15–54.
- (56) Golas, P. L.; Matyjaszewski, K. Marrying click chemistry with polymerization: expanding the scope of polymeric materials. *Chem. Soc. Rev.* **2010**, *39*, 1338–1354.
- (57) Xi, W.; Scott, T. F.; Kloxin, C. J.; Bowman, C. N. Click Chemistry in Materials Science. *Adv. Funct. Mater.* **2014**, 24, 2572–2590.
- (58) Howe, D. H.; McDaniel, R. M.; Magenau, A. J. D. From Click Chemistry to Cross-Coupling: Designer Polymers from One Efficient Reaction. *Macromolecules* **2017**, *50*, 8010–8018.
- (59) Howe, D. H.; Jenewein, K. J.; Hart, J. L.; Taheri, M. L.; Magenau, A. J. D. Functionalization-induced self-assembly under ambient conditions via thiol-epoxide "click" chemistry. *Polym. Chem.* **2019**, *11*, 298–303.
- (60) Magenau, A. J. D.; Chan, J. W.; Hoyle, C. E.; Storey, R. F. Facile polyisobutylene functionalization via thiol-ene click chemistry. *Polym. Chem.* **2010**, *1*, 831–833.
- (61) Wilson, O. R.; McDaniel, R. M.; Rivera, A. D.; Magenau, A. J. D. Alkylborane-Initiated Thiol-Ene Networks for the Synthesis of Thick and Highly Loaded Nanocomposites. *ACS Appl. Mater. Interfaces* **2020**, *12*, 55262.
- (62) Shin, J.; Matsushima, H.; Chan, J. W.; Hoyle, C. E. Segmented Polythiourethane Elastomers through Sequential Thiol—Ene and Thiol—Isocyanate Reactions. *Macromolecules* **2009**, 42, 3294—3301.
- (63) Magenau, A. J. D.; Hartlage, T. R.; Storey, R. F. Thiolterminated polyisobutylene: Synthesis, characterization, and derivatization. J. Polym. Sci., Part A: Polym. Chem. 2010, 48, 5505-5513.
- (64) Li, H.; Yu, B.; Matsushima, H.; Hoyle, C. E.; Lowe, A. B. The Thiol–Isocyanate Click Reaction: Facile and Quantitative Access to ω-End-Functional Poly(N,N-diethylacrylamide) Synthesized by RAFT Radical Polymerization. *Macromolecules* **2009**, 42, 6537–6542.
- (65) Hensarling, R. M.; Rahane, S. B.; LeBlanc, A. P.; Sparks, B. J.; White, E. M.; Locklin, J.; Patton, D. L. Thiol—isocyanate "click" reactions: rapid development of functional polymeric surfaces. *Polym. Chem.* **2011**, *2*, 88–90.
- (66) Li, C.; Tan, J.; Li, H.; Yin, D.; Gu, J.; Zhang, B.; Zhang, Q. Thiol—isocyanate click reaction in a Pickering emulsion: a rapid and efficient route to encapsulation of healing agents. *Polym. Chem.* **2015**, *6*, 7100–7111.
- (67) Droger, N.; Primel, O.; Halary, J. L. Characterization of the viscoelastic and mechanical properties of tightly cross-linked polythiourethane networks. *J. Appl. Polym. Sci.* **2008**, *107*, 455–462.
- (68) Hoyle, C. E.; Lowe, A. B.; Bowman, C. N. Thiol-click chemistry: a multifaceted toolbox for small molecule and polymer synthesis. *Chem. Soc. Rev.* **2010**, *39*, 1355–1387.
- (69) Li, L.; Chen, X.; Torkelson, J. M. Reprocessable Polymer Networks via Thiourethane Dynamic Chemistry: Recovery of Crosslink Density after Recycling and Proof-of-Principle Solvolysis Leading to Monomer Recovery. *Macromolecules* **2019**, *52*, 8207–8216.
- (70) Wen, Z.; Han, X.; Fairbanks, B. D.; Yang, K.; Bowman, C. N. Development of thiourethanes as robust, reprocessable networks. *Polymer* **2020**, 202, 122715.

- (71) Stankovich, S.; Dikin, D. A.; Dommett, G. H. B.; Kohlhaas, K. M.; Zimney, E. J.; Stach, E. A.; Piner, R. D.; Nguyen, S. T.; Ruoff, R. S. Graphene-based composite materials. *Nature* **2006**, 442, 282–286.
- (72) Stankovich, S.; Piner, R. D.; Nguyen, S. T.; Ruoff, R. S. Synthesis and exfoliation of isocyanate-treated graphene oxide nanoplatelets. *Carbon* **2006**, *44*, 3342–3347.
- (73) Althues, H.; Henle, J.; Kaskel, S. Functional inorganic nanofillers for transparent polymers. *Chem. Soc. Rev.* **2007**, *36*, 1454–1465.
- (74) Kango, S.; Kalia, S.; Celli, A.; Njuguna, J.; Habibi, Y.; Kumar, R. Surface modification of inorganic nanoparticles for development of organic—inorganic nanocomposites—A review. *Prog. Polym. Sci.* **2013**, 38, 1232—1261.
- (75) Ghidiu, M.; Halim, J.; Kota, S.; Bish, D.; Gogotsi, Y.; Barsoum, M. W. Ion-Exchange and Cation Solvation Reactions in Ti<sub>3</sub>C<sub>2</sub> MXene. *Chem. Mater.* **2016**, 28, 3507–3514.
- (76) Ghidiu, M.; Kota, S.; Halim, J.; Sherwood, A. W.; Nedfors, N.; Rosen, J.; Mochalin, V. N.; Barsoum, M. W. Alkylammonium Cation Intercalation into Ti3C2 (MXene): Effects on Properties and Ion-Exchange Capacity Estimation. *Chem. Mater.* **2017**, *29*, 1099–1106.
- (77) Silverstein, R. M.; Webster, F. S.; Kiemle, D. J. Spectrometric Identification of Organic Compounds, 7 ed.; John Wiley & Sons, Inc, 2005; p 502.
- (78) Danon, A.; Stair, P. C.; Weitz, E. FTIR Study of CO<sub>2</sub> Adsorption on Amine-Grafted SBA-15: Elucidation of Adsorbed Species. *J. Phys. Chem. C* **2011**, *115*, 11540–11549.
- (79) Lv, S.; Zhou, W.; Li, S.; Shi, W. A novel method for preparation of exfoliated UV-curable polymer/clay nanocomposites. *Eur. Polym. J.* **2008**, *44*, 1613–1619.
- (80) Davidson, B. J.; Gee, S. J.; Hurst, G. C.; Rucker, J. B.; Shouse, J. L.; Smith, J. B.; Cavitt, T. B. Covalently bound organomodified clay photoinitiators. *J. Appl. Polym. Sci.* **2015**, *132*, 41883.
- (81) Ou, B.; Li, D.; Liu, Q.; Zhou, Z.; Chen, G.; Liu, P. Preparation of Conductive Polyaniline/Functionalized Titanium Dioxide Nanocomposites via Graft Polymerization. *J. Macromol. Sci., Part A: Pure Appl.Chem.* **2012**, *49*, 149–153.
- (82) Delebecq, E.; Pascault, J.-P.; Boutevin, B.; Ganachaud, F. On the Versatility of Urethane/Urea Bonds: Reversibility, Blocked Isocyanate, and Non-isocyanate Polyurethane. *Chem. Rev.* **2013**, 113, 80–118
- (83) Persson, P. O. Å.; Rosen, J. Current state of the art on tailoring the MXene composition, structure, and surface chemistry. *Curr. Opin. Solid State Mater. Sci.* **2019**, 23, 100774.
- (84) Ibragimova, R.; Puska, M. J.; Komsa, H.-P. pH-Dependent Distribution of Functional Groups on Titanium-Based MXenes. *ACS Nano* **2019**, *13*, 9171–9181.
- (85) Hu, T.; Hu, M.; Gao, B.; Li, W.; Wang, X. Screening Surface Structure of MXenes by High-Throughput Computation and Vibrational Spectroscopic Confirmation. *J. Phys. Chem. C* **2018**, 122, 18501–18509.
- (86) Persson, I.; Näslund, L.-Å.; Halim, J.; Barsoum, M. W.; Darakchieva, V.; Palisaitis, J.; Rosen, J.; Persson, P. O. Å. On the organization and thermal behavior of functional groups on  ${\rm Ti_3C_2}$  MXene surfaces in vacuum. 2D Mater. 2017, 5, 015002.
- (87) Hu, M.; Hu, T.; Li, Z.; Yang, Y.; Cheng, R.; Yang, J.; Cui, C.; Wang, X. Surface Functional Groups and Interlayer Water Determine the Electrochemical Capacitance of Ti<sub>3</sub>C<sub>2</sub>T<sub>x</sub> MXene. *ACS Nano* **2018**, *12*, 3578–3586.
- (88) Halim, J.; Cook, K. M.; Naguib, M.; Eklund, P.; Gogotsi, Y.; Rosen, J.; Barsoum, M. W. X-ray photoelectron spectroscopy of select multi-layered transition metal carbides (MXenes). *Appl. Surf. Sci.* **2016**, 362, 406–417.
- (89) Hope, M. A.; Griffith, K. J.; Ghidiu, M.; Grey, C. P.; Gogotsi, Y. NMR reveals the surface functionalisation of Ti<sub>3</sub>C<sub>2</sub> MXene. *Phys. Chem. Chem. Phys.* **2016**, *18*, 5099–5102.
- (90) Fan, C.-J.; Wen, Z.-B.; Xu, Z.-Y.; Xiao, Y.; Wu, D.; Yang, K.-K.; Wang, Y.-Z. Adaptable Strategy to Fabricate Self-Healable and Reprocessable Poly(thiourethane-urethane) Elastomers via Reversible

- Thiol-Isocyanate Click Chemistry. *Macromolecules* **2020**, *53*, 4284–4293.
- (91) Gamardella, F.; De la Flor, S.; Ramis, X.; Serra, A. Recyclable poly(thiourethane) vitrimers with high Tg. Influence of the isocyanate structure. *React. Funct. Polym.* **2020**, *151*, 104574.
- (92) Becker, C.; Krug, H.; Schmidt, H. Tailoring of Thermomechanical Properties of Thermoplastic Nanocomposites by Surface Modification of Nanoscale Silica Particles. *MRS Online Proc. Libr.* **1996**, 435, 237.
- (93) Ash, B. J.; Schadler, L. S.; Siegel, R. W. Glass transition behavior of alumina/polymethylmethacrylate nanocomposites. *Mater. Lett.* **2002**, *55*, 83–87.
- (94) Bansal, A.; Yang, H.; Li, C.; Cho, K.; Benicewicz, B. C.; Kumar, S. K.; Schadler, L. S. Quantitative equivalence between polymer nanocomposites and thin polymer films. *Nat. Mater.* **2005**, *4*, 693–698.
- (95) Throckmorton, J.; Palmese, G. Direct Preparation of Few Layer Graphene Epoxy Nanocomposites from Untreated Flake Graphite. *ACS Appl. Mater. Interfaces* **2015**, *7*, 14870–14877.
- (96) Shtein, M.; Nadiv, R.; Lachman, N.; Daniel Wagner, H.; Regev, O. Fracture behavior of nanotube—polymer composites: Insights on surface roughness and failure mechanism. *Compos. Sci. Technol.* **2013**, 87, 157–163.
- (97) Wu, S.-H.; Wang, F.-Y.; Ma, C.-C. M.; Chang, W.-C.; Kuo, C.-T.; Kuan, H.-C.; Chen, W.-J. Mechanical, thermal and morphological properties of glass fiber and carbon fiber reinforced polyamide-6 and polyamide-6/clay nanocomposites. *Mater. Lett.* **2001**, *49*, 327–333.